ELSEVIER

Applied Surface Science 182 (2001) 150–158

applied surface science

www.elsevier.com/locate/apsusc

Highly *c*-axis oriented $LiNb_{0.5}Ta_{0.5}O_3$ thin films on Si substrates fabricated by thermal plasma spray CVD

S.A. Kulinich[a,*], J. Shibata[b], H. Yamamoto[c], Y. Shimada[c], K. Terashima[a,c], T. Yoshida[a]

[a]*Department of Materials Engineering, Faculty of Engineering, The University of Tokyo, 7-3-1 Hongo, Bunkyo-ku, 113-8656 Tokyo, Japan*
[b]*Engineering Research Institute, School of Engineering, The University of Tokyo, 2-11-16 Yayoi, Bunkyo-ku, 113-8656 Tokyo, Japan*
[c]*Department of Advanced Materials Science, Graduate School of Frontier Science, The University of Tokyo, 7-3-1 Hongo, Bunkyo-ku, 113-8656 Tokyo, Japan*

Received 22 May 2001; received in revised form 30 July 2001; accepted 10 August 2001

Abstract

Lithium niobate-tantalate films with the composition $LiNb_{0.5}Ta_{0.5}O_3$ and very high *c*-axis orientation were grown on (1 0 0) and (1 1 1) Si substrates by using the thermal plasma spray CVD method. It is demonstrated that the substrate temperature is the key factor governing film orientation and crystallinity. The film direction could be varied from (0 0 6) to (0 1 2) by controlling the deposition temperature. Under optimal growth conditions, 97% *c*-textured films could be grown on both thick and very thin intermediate SiO_2 layers. A (0 0 6) rocking-curve full-width at half-maximum value could achieve 3.7° by using the optimal deposition temperature. The growth rate applied was equal to 160–340 nm/min. © 2001 Published by Elsevier Science B.V.

PACS: 81.15.Gh; 68.55.-a

Keywords: $LiNb_{0.5}Ta_{0.5}O_3$; Thin films; Thermal plasma spray CVD; X-ray diffraction

1. Introduction

Ferroelectric oxide thin films have been attracting great interest for various applications, including non-volatile memory, infrared sensors, optical switches and ultrasonic transducers. To take advantage of the useful properties of these materials, it is essential to fabricate epitaxial or polar-axis-oriented thin films [1,2]. Optical devices require epitaxial films, whereas preferentially oriented ferroelectric films are sufficient for many piezoelectric device applications.

Lithium niobate ($LiNbO_3$, LN) and lithium tantalate ($LiTaO_3$, LT) are ferroelectric materials with various attractive properties, such as acoustic, piezoelectric, acoustooptic and electrooptic properties [3,4]. Recently, high-quality LN and LT thin films have been receiving great attention for their applications in optical waveguide devices, such as wave mixing, intensity phase modulation and high-speed switching in integrated optics [5].

In contrast, there have been only a few reports on lithium niobate-tantalate ($LiNb_{1-x}Ta_xO_3$, LNT) film deposition [6–8], even though this material is also very attractive, since its properties can be varied along with x from those of LN ($x = 0$) to those of LT ($x = 1$). Kawaguchi et al. [6] reported LNT film growth on

* Corresponding author. Tel./fax: +81-3-5841-7103.
E-mail address: kulinich@terra.mm.t.u-tokyo.ac.jp (S.A. Kulinich).

0169-4332/01/$ – see front matter
PII: S0169-4332(01)00523-2

LN(0 0 1) substrates with $x = 0$–0.4 using the LPE method. In their experiment, film crystallinity (FWHM) degraded markedly when $x > 0.3$, corresponding to the increase of lattice mismatch and growth temperature. Cheng et al. [7] prepared highly (0 0 6)-oriented LNT films with $x < 0.33$ on Si(1 1 1) substrates using the sol–gel technique. They also found that the degree of orientation was relatively low when $0.5 < x < 1$.

From the technological point of view, $LiNb_{1-x}Ta_xO_3$ ($x = 0$–1) films on silicon or other semiconductors are very desirable, because they would enable an integrated optics technology in which sources, detectors, electronics and nonlinear optical waveguides could be fabricated on a single substrate. To exploit the optical properties of these materials and the superior electrical properties of silicon, it is of great importance to fabricate highly *c*-textured LNT films on Si substrates, for both metal-ferroelectric-semiconductor nonvolatile memory and optoelectronic applications [2,7].

Recently, many authors have reported depositing LN and LT films with (1 0 4) [9,10], (0 1 2) [11] and (0 0 6) [2,12–18] texture on Si with/without a SiO_2 cladding layer, using PLD [2,10,15,17,18], sputtering [9,12], the sol–gel technique [13], the pyrosol method [14] and MO CVD [11,16]. However, there is little information on the crystallinity of these films [16], and there are only a few reports on LNT films on Si substrate [7].

The thermal plasma spray CVD (TPS CVD) technique using liquid source material [19] has been successfully applied to the preparation of preferentially (1 1 0)-oriented LN films onto (1 1 0) sapphire with the deposition rate as high as 0.1 μm/min, which was 10–100 times faster than those of many other conventional vapor deposition methods. The authors have also reported depositing LN on a 5 in. Si(1 1 1) wafer [19]. Since the substrate temperature could not be controlled in that experiment, different film quality and orientation were obtained for various substrate areas. It has recently been demonstrated that epitaxial $LiNb_{1-x}Ta_xO_3$ ($x = 0$–0.7) films with good crystallinity can be grown on (0 0 1) sapphire substrates using the same method [8,20,21]. In the present paper, we report on $LiNb_{0.5}Ta_{0.5}O_3$ thin films (160–340 nm) fabricated on Si(1 1 1) and Si(1 0 0) substrates by the same deposition technique. In particular, the effects of deposition temperature and cladding SiO_2 layer thickness on film orientation and crystallinity have been investigated.

2. Experimental details

The double-alkoxide liquid precursors were reagent-grade lithium-niobium and lithium-tantalum alkoxide metalorganic solutions commercially available for dip coating {$LiNb(OR)_6$ and $LiTa(OR)_6$ in 3-methylbutylacetate as a solvent} from Kojundo Chemical, Japan. The concentrations of metals (Li and Nb or Li and Ta) in individual precursor solutions, which were then mixed in appropriate ratios, corresponded to 3 wt.% $LiNbO_3$ or 3 wt.% $LiTaO_3$, respectively. In earlier works, we reported that a mixture of these solutions with the initial ratio Nb:Ta = 1:1 yielded single-phase LNT (with x of approximately 0.5) on sapphire substrates [8,20,21], and this source composition was used here.

A TPS CVD apparatus with upward-blowing plasma, described previously [8,20], was used in this study. The main details of the method, as well as the deposition procedure itself, have also been described elsewhere [8,19,20]. Unlike in our previous studies [8,20,21], we used a modified TPS CVD apparatus, in which the auxiliary Cu inductive coil for holder heating (independent of plasma heating) was added (Fig. 1). Whereas in previous studies, the substrate

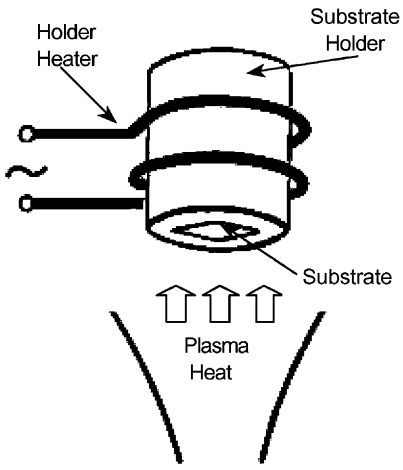

Fig. 1. Scheme of the improved substrate heating system of the TPS CVD apparatus depicting independent holder heating by both auxiliary Cu inductive coil and plasma with fixed power.

Table 1
Summary of experimental conditions

Source Li:Nb:Ta ratio	2:1:1
Power (kW)	46.2
Pressure (Torr)	150
O_2 tangential gas flow rate (l/min)	45.0
Ar carrier gas flow rate (l/min)	3.0
Ar spray gas flow rate (l/min)	3.6
Ar inner gas flow rate (l/min)	5.0
Liquid feeding rate, R (ml/min)	4.0, 8.0
Deposition temperature (°C)	560–700
Torch-substrate distance, L (cm)	37
Deposition time (s)	30–60
Substrates	Si (1 1 1), Si (1 0 0)
SiO_2 cladding layer thickness (nm)	10, 600, 700, 900

temperature was controlled within the accuracy of ±15°C [8,20,21], the improved heating system depicted in Fig. 1 enabled us to keep T_{sub} within the accuracy of ±5 and ±10°C at liquid precursor feeding rates $R = 4$ and 8 ml/min, respectively.

A summary of the main experimental conditions is presented in Table 1. Silicon plates ($10 \times 10 \times 0.5\,mm^3$ in size, Si(1 0 0) or Si(1 1 1) p-type) were used as substrates. Since the refractive index of Si ($n = 3.42$) is greater than those of $LiNb_{1-x}Ta_xO_3$ (at. $\lambda = 632.8$ nm and $x = 0.81$: $n_o = 2.20$, $n_e = 2.19$), the LNT/Si waveguide structure requires a sufficiently thick buffer layer with a smaller index and low loss in the visible area in order to confine the optical power in the waveguide and to reduce the leakage loss to a negligible value [9,15,16]. For this purpose, an amorphous SiO_2 layer seems to be very advantageous, because it is very common in semiconductor processing, is easily grown by thermal oxidizing and has a low refractive index ($n = 1.46$). To fabricate a SiO_2 buffer layer, a number of Si wafers were heat-treated in a quartz pipe at 1100°C and oxygen flow for 20, 27 and 47 h, so that samples with coating thicknesses of 600, 700 and 900 nm were obtained. Prior to film growth, the Si wafers were ultrasonically cleaned and rinsed with acetone and ethanol. Additionally, a number of Si plates with a natural SiO_2 layer of approximately 10 nm were used as substrates for comparison.

In order to examine the LNT film orientation, crystallinity and phase composition, X-ray diffraction (XRD) was used. Film and SiO_2 cladding layer thicknesses were examined by cross-sectional scanning electron microscopy (SEM) and transmission electron microscopy (TEM). Surface morphology was analyzed with SEM and atomic force microscopy (AFM). The microstructure and interface between the film and the substrate were studied using TEM, energy-dispersive X-ray spectroscopy (EDS) with a probe of 2 nm size was applied to determine the chemical composition of the films. The refractive index was evaluated by means of spectroscopic ellipsometry.

3. Results and discussion

3.1. Orientation and crystallinity

To study the effect of deposition temperature on film orientation and crystallinity, only the substrate temperature T_{sub} was varied in the experiments shown in Fig. 2. The phase composition and crystallite orientation of the LNT/SiO_2/Si films were analyzed by XRD using a θ–2θ scanning mode; the θ scanning mode was used to estimate film (0 0 6) out-of-plane misalignment (rocking-curve measurement). Since

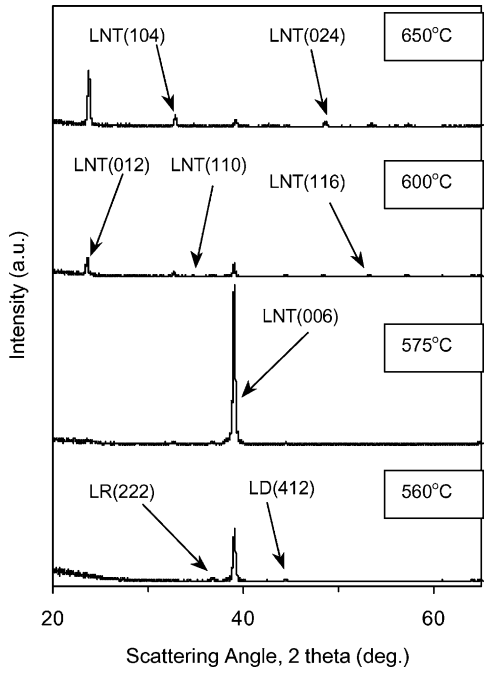

Fig. 2. Variation of XRD patterns of $LiNb_{0.5}Ta_{0.5}O_3$ films deposited on SiO_2/Si (oxide thickness about 900 nm) substrates with deposition temperature T_{sub}.

these XRD results are affected by film thickness, all the series were grown to have similar thicknesses of 160–180 nm. The substrates used were (1 0 0)Si covered with a 900 nm thick oxide layer, and the liquid feeding rate was maintained at $R = 4\,\mathrm{ml/min}$, which corresponded to the film growth rate of 160–180 nm/min. The LNT films were deposited within the T_{sub} range 560–700°C for 1 min and were then in situ annealed in O_2/Ar plasma at the deposition temperature for 10 min.

Fig. 2 shows the variation of the LNT film XRD patterns with the deposition temperature. At $T_{sub} = 560$°C, highly (0 0 6)-oriented film was grown; however, the intensity of the (0 0 6) peak is rather weak. Also, a weak (2 2 2) peak of the Li-rich phase ($Li_3Nb_{0.5}Ta_{0.5}O_4$, LR) near $2\theta = 37°$, as well as a set of very weak peaks of the Li-deficient phase ($LiNb_{1.5}Ta_{1.5}O_8$, LD) were observed. The latter are believed to result from the fast deposition and relatively low species mobility in this temperature range, where some compositional and phase inhomogeneities can form. At elevated deposition temperatures, the surface mobility and volume diffusion became faster, which resulted in the decrease of the LR and LD peak intensities and better film compositional homogeneity. For the same reason, in situ O_2/Ar plasma annealing was used to increase film crystallinity and phase homogeneity. Note that the formation of the (1 1 1)-oriented LR phase following LN deposition on sapphire or Si substrates has been reported previously [22,23].

At higher T_{sub}, the (0 0 6) peak intensity increased until about 575°C; at this temperature, 97% *c*-axis oriented LNT film could be grown (see Figs. 2 and 3). When deposition temperatures increased to higher than 580°C, a gradual decrease of the (0 0 6) peak intensity, along with an increase of those for (0 1 2), (1 0 4), (1 1 0), (2 0 2), (0 2 4), (1 1 6) and (3 0 0) peaks, was observed. Thus, the XRD patterns in Fig. 2 clearly show that highly *c*-axis oriented LNT films could be grown by using an appropriate substrate temperature. At $T_{sub} = 650-700$°C, LNT films with polycrystalline orientation and XRD spectra, similar to those for powder data, were fabricated.

Since no particular lattice relationship is expected between LNT and Si or SiO_2 in this *c*-axis orientation, it is clear that such a strong texture arises principally from the growth kinetics of the highly anisotropic

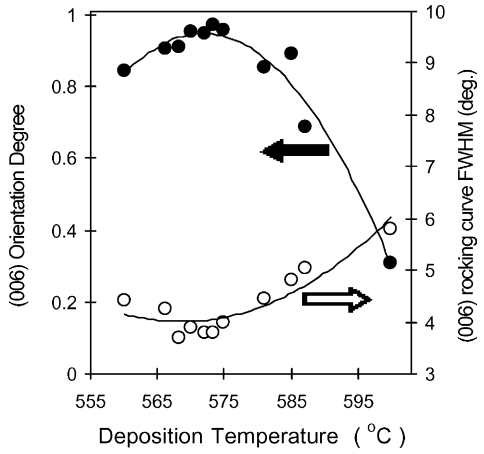

Fig. 3. Variation of orientation degree (*f*) for $LiNb_{0.5}Ta_{0.5}O_3$ (160–180 nm thick) films as a function of deposition temperature T_{sub} (the change of the (0 0 6) rocking-curve FWHM value for the same films is also shown).

LNT material. In principle, film orientation during deposition may result from either surface free energy or growth-rate anisotropy effects [16].The *c*-axis is well known to be the fastest growth direction for LNT, so that when formed, *c*-axis textured LNT grains can consume most ad-species before the other grains can grow [16]. Moreover, at lower temperatures, since the lateral growth of grains is relatively slow compared to their vertical growth rate, growth is dominated by islands with their fastest growth direction normal to the film plane. Thus, the high (0 0 6) LNT film orientation at $T_{sub} = 560-575$°C (Fig. 2) resulted from the fast growth rate of the *c*-axis (growth-rate anisotropy).

The gradual change in texture with deposition temperature could be explained by surface free energy anisotropy. Wu et al. [24] have suggested that the (0 1 2) plane is the lowest energy plane. At higher temperatures, nuclei on the surface can rearrange themselves to minimize the total surface energy, thus (0 1 2) orientation rather than (0 0 6) is favorable [16].

It is noteworthy that a very similar tendency in LN/SiO_2/Si film texturing with deposition temperatures was reported by Lee and Feigelson [16]. In their MO CVD experiment, when a faster growth rate (4.5–5.5 nm/min) was used, *c*-axis orientation could be maintained at higher temperatures, and the formation of the (0 1 2) texture was significantly retarded compared to the slower growth rates (1.0–1.5 nm/min).

Since the film growth rates in our experiments were 30–60 times higher than those in their work, the change in texture would be expected at higher deposition temperatures. However, it was not observed in this study, and highly (0 0 6)-oriented LNT films could be deposited within a relatively narrow temperature range around 567–580°C for both $R = 4$ and 8 ml/min, which can be attributed to the contribution of a number of factors, such as the influence of apparatus geometry and deposition conditions. For example, less reliable temperature control in the case of the higher feeding rate, $R = 8\,\mathrm{ml/min}$ (± 10°C, whereas ± 5°C at $R = 4\,\mathrm{ml/min}$), is believed to be one of the possible reasons why the LNT film orientation and crystallinity could not be improved using a higher growth rate.

According to Hu et al. [17], a convenient parameter for describing the degree of *c*-axis orientation of the LNT films (*c*-axis orientation degree) on Si substrates can be defined as

$$f = \frac{I_r(0\,0\,6) - I_r^{\mathrm{powder}}(0\,0\,6)}{1 - I_r^{\mathrm{powder}}(0\,0\,6)},$$

where relative intensity $I_r(0\,0\,6)$ is the intensity of the (0 0 6) peak normalized by the sum intensity of all the peaks of LNT between $2\theta = 20$ and 60°. For randomly oriented polycrystalline films, as in the case of powders, the degree of *c*-axis orientation (f) is equal to 0; for completely *c*-axis oriented LNT films, $f = 1$; and for partially *c*-axis oriented films, f falls between 0 and 1 [7,13,17,20]. In the present study, we extended the angle range to $2\theta = 20{-}70°$ so as to include the effect of the LNT (3 0 0) plane as well.

The change in LNT film orientation degree as a function of growth temperature is presented in Fig. 3; the change in the film crystallinity ((0 0 6) rocking-curve FWHM value) is also indicated. These two relationships were carefully obtained using XRD with both 2θ–θ and θ (rocking-curve) measurements. The LNT films used to obtain these dependencies were the same series as those shown in Fig. 2. As shown in Fig. 3, both film texturing (orientation factor f) and crystallinity were found to increase with increasing deposition temperature until approximately 575°C, indicating better *c*-axis crystalline alignment, caused by increasing diffusion and surface mobility. These results were expected, because the *c*-axis orientation was improved until this temperature was reached, as discussed earlier and shown in Fig. 2. When the deposition temperature exceeded $T_{sub} = 575$°C, the gradual rise of the (0 0 6) rocking-curve FWHM value, as well as the gradual decrease of the LNT film orientation degree, were observed, indicating the change of the (0 0 6) texturing to the (0 1 2) one. The narrowest (0 0 6) rocking-curve FWHM width achieved in this work was equal to 3.7°.

To date, the narrowest rocking-curve FWHM value that has been reported for the LN films grown on SiO_2/Si or Si is equal to 1.8° [16]. Although our best value for LNT film is still large, we consider it to be rather good, taking into account the very high deposition rate applied in our study and the fact that in situ annealing temperatures and times were not optimized.

Although a single-crystalline film would be of more interest, it is sufficient for many nonlinear optical applications that the LNT film be *c*-axis oriented, since the *c*-axis direction is the optical axis of the crystal, and the *c*-textured film gives a single d_{33} coefficient for the entire film. Thus, the *c*-axis oriented but polycrystalline LNT films described here are believed to meet the criteria for crystalline quality required for nonlinear optical and electrooptical devices.

In many works, the deposition of highly *c*-axis oriented LN or LT films on Si has been achieved only by using SiN_x [23], Al_2O_3 [17], LT [12] or SiO_2 [14] buffer layers or an additional electric field applied normal to the substrate during film growth [15,18,24]. In other cases, fused silica [24] or a thick (1800 nm) SiO_2 layer [2] were used for the same purpose. In contrast, in our study, highly *c*-axis oriented LNT films were fabricated on Si with both a native thin and thermally grown thick SiO_2 substrates.

3.2. Interface and chemical composition

From SEM and TEM analyses, it can be found that the majority of LNT films exhibited the columnar growth mode. The crystallites observed confirmed the strong *c*-axis orientation, although the in-plane alignment was random for different grains. Also, no secondary phase was detected by TEM near the interface vicinity, although some amount of amorphous phase was found between LNT grains, implying that growth and annealing conditions can be further optimized.

Fig. 4a shows a cross-sectional TEM micrograph revealing the interface structure of LNT film on silicon

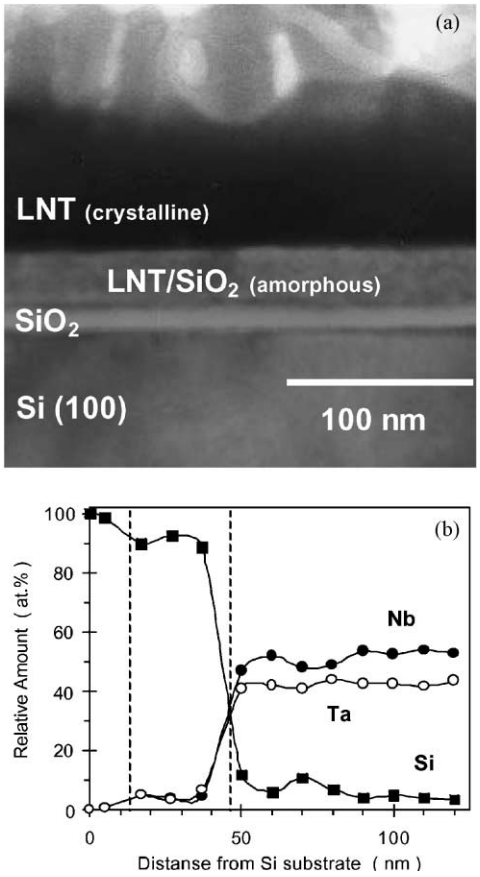

Fig. 4. (a) Typical cross-sectional TEM micrograph showing the interface between the 170 nm thick $LiNb_{0.5}Ta_{0.5}O_3$ film deposited at $R = 4\,ml/min$ for 1 min onto the Si(1 0 0) substrate without the previously formed SiO_2 cladding interlayer. (b) Variation of Si, Nb and Ta contents across the interface of the same sample, as measured by EDS analysis; SiO_2, amorphous LNT/SiO_2 and crystalline LNT areas are separated by dashed lines.

substrate with native SiO_2 only. A number of layers with distinct boundaries are visible, namely, amorphous SiO_2, an amorphous LNT/SiO_2 intermediate layer and the crystalline LNT film itself. It should be noted that a very similar interface structure was observed for a film deposited onto a Si(1 0 0) wafer covered with a 600 nm thick SiO_2 cladding layer (or 700/900 nm thick), where an amorphous intermediate layer of 30–35 nm between the SiO_2 and LNT crystalline film was also found. This implies that the SiO_2 thickness does not affect the thickness of such an intermediate amorphous layer, which is in accordance with the results described above. A similar amorphous intermediate layer of 5–10 nm in thickness has been reported by Lee and Feigelson [16] for their MO CVD-fabricated LN films on SiO_2/Si substrates.

Fig. 4b shows the variation of Si, Nb and Ta contents across the interface of the same sample, as measured by EDS analysis; amorhpous SiO_2, amorphous LNT/SiO_2 and crystalline LNT areas are separated by dashed lines, corresponding to those in Fig. 4a. As is evident, Si, Nb and Ta atoms are distributed in accordance with the diffusion profiles shown in Fig. 4b. As the accuracy of this analytical method is approximately ± 5 at.%, it can be considered that $LiNb_{1-x}Ta_xO_3$ films with Ta content $x = Ta/(Nb + Ta)$ close to 0.5 were fabricated, which is in good agreement with our previous results on sapphire substrates [8,20,21].

In order to clarify the structure of the interface between the LNT film and the surface of Si substrate in more detail, a thorough HR TEM examination was performed. The HR TEM micrograph of Fig. 5 shows the detailed structure of the part of the intermediate layer consisting of SiO_2 and LNT, according to Fig. 4b. Although the intermediate LNT/SiO_2 layer

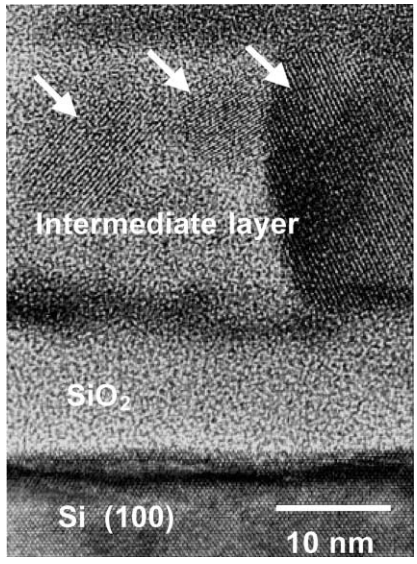

Fig. 5. A cross-sectional HR TEM image for the $LiNb_{0.5}Ta_{0.5}O_3$ film deposited onto a Si(1 0 0) substrate with a native SiO_2 layer. Only interface areas including Si, SiO_2 and the amorphous intermediate layer of approximately 30 nm are shown. One large and two smaller LNT crystallites within the latter are depicted with white arrows.

mainly has an amorphous nature, some crystalline LNT grains can be found there, as shown in Fig. 5. Note that the larger crystallite on the right-hand side of Fig. 5 appears to have a direct relationship with the amorphous SiO_2 cladding layer, implying that, under some conditions, there could be a direct growth of LNT crystalline film on amorphous SiO_2 layer without any amorphous intermediate layer. This is not in keeping with the results of Lee and Feigelson [16], but agrees well with those of Ghica et al. [10], whose PLD-fabricated LN film cross-sectional TEM revealed no amorphous intermediate layer within the interface. While Lee and Feigelson assumed that some Li atoms existed within the LN/SiO_2 intermediate layer, in this study, LNT crystallites were clearly observed to be included in the interlayer mentioned above. It is believed that better control of this layer thickness and structure will positively affect the LNT film quality and properties.

The hexagonal *c*-lattice parameter for the LNT films calculated from the XRD patterns (based on the (0 0 6)-planes) was equal to 13.81–13.83 Å, which is close to the datum for the bulk $LiNb_{0.5}Ta_{0.5}O_3$ (13.815 Å, PDF No. 38-1252). Our results for the LNT *c*-parameter are in reasonable agreement with those of Cheng et al. [7], who reported $c = 13.84$ Å for the sol–gel-derived $LiNb_{0.5}Ta_{0.5}O_3$ films on Si(1 1 1) substrates, although they differ from the results of Bornand et al. [14], whose pyrosol-deposited LT films on Si(1 1 1) were weakly compressed along the *c*-axis. Note that TPS-CVD-fabricated epitaxial $LiNb_{0.5}Ta_{0.5}O_3$ films on (0 0 1) sapphire had smaller *c*-parameters of 13.75–13.77 Å, which is believed to be due to the effect of planar tensile stress resulting from the difference in the thermal expansion coefficients of the film and substrate [8,20,21].

3.3. Film thickness and surface morphology

For LNT films deposited at liquid feeding rates $R = 4$ and 8 ml/min, the growth rates estimated from cross-sectional SEM images were the values of 160–180 and 300–340 nm/min, respectively.

SEM and AFM surface images of mirror-like LNT films on SiO_2/Si substrates revealed that their surface did not contain any cracks or other serious defects. The LNT film surface morphology for the sample deposited at $T_{sub} = 570°C$ and $R = 4\,ml/min$ for 1 min, observed by AFM, is presented in Fig. 6. However, as demonstrated in our previous works [8,20], the roughness of the high-growth-rate-deposited LNT films by TPS CVD is somewhat higher than that of the LN and LT films with the best surface. Therefore, further experimental studies on nucleation and growth mechanisms are necessary in order to decrease the grain size and improve the surface morphology of the LNT films produced. As it was reported previously [16,25] the source material input *R* increase may lead to some reduction in grain size, which, in principle, can make the film surface smoother by decreasing the depth of grain-boundary grooves. It implies that controlling the growth rate (source feeding rate) may be a key factor in varying the LNT film surface morphology.

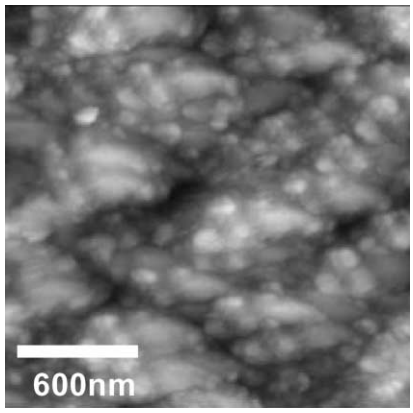

Fig. 6. Surface morphology of the 170 nm thick $LiNb_{0.5}Ta_{0.5}O_3$ film deposited at $R = 4\,ml/min$ for 1 min onto Si(1 0 0) substrate with previously formed 900 nm thick SiO_2 buffer layer. $T_{sub} = 570°C$; (0 0 6) rocking curve FWHM value 4.2°C; rms roughness 14 nm.

3.4. Refractive index

Fig. 7 shows the refractive index dependence on wavelength, evaluated from the ellipsometric measurements of the approximately 300 nm thick film, deposited at $R = 8\,ml/min$ for 30 s onto a Si(1 1 1) substrate covered with a SiO_2 cladding layer on the order of 700 nm thickness. After deposition, the film was in situ annealed by oxygen plasma at 575°C for 5 min. Its (0 0 6) rocking-curve FWHM value was approximately 4.2°. Ellipsometric method does not allow the separation of the two indices of anisotropic

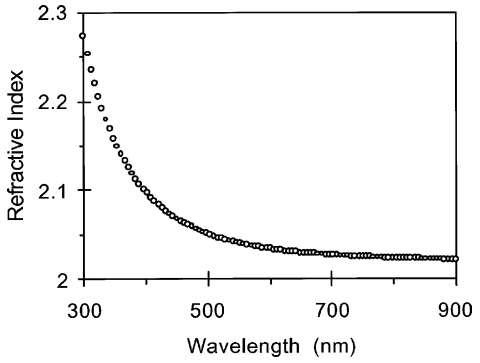

Fig. 7. Refractive index for a 300 nm thick $LiNb_{0.5}Ta_{0.5}O_3$ film deposited onto a SiO_2/Si(1 1 1) substrate (oxide thickness about 700 nm) at $R = 8$ ml/min, measured by spectroscopic ellipsometry.

LNT material, n_o (ordinary index) and n_e (extraordinary index), which are in the direction normal to the *c*-axis and along the *c*-axis, respectively.

For the crystal composition $LiNb_{0.5}Ta_{0.5}O_3$, experimental values of the refractive indices have not been reported so far. Xue et al. [26] calculated the refractive indices of $LiNb_{1-x}Ta_xO_3$ for the crystal compositions ($x = 0.81$, 0.92, and 0.97) for which experimental values have already been reported [27]. From their linear fit, the numerical dependence of n_o on the Ta content can be derived to be $n_o = 2.23 - 0.19x$, which gives 2.135 for $x = 0.5$ (note that the equation gives the n_o value at.$\lambda = 1064$ nm).

It should be mentioned that, in general, the refractive index is mainly influenced by the crystallinity and density of the film. Therefore, somewhat lower indices of the film suggest the presence of amorphous or not well-crystallized regions in this sample, which is in agreement with the TEM observations. However, this result is rather promising, considering that the crystallinity and density of TPS-CVD-fabricated films can probably be improved by using better deposition temperature control, in situ annealing conditions and controlling the thickness and structure of the amorphous intermediate layer.

4. Conclusions

For the first time, lithium niobate-tantalate films with the composition $LiNb_{0.5}Ta_{0.5}O_3$ and with very high *c*-axis orientation have been grown on both (1 0 0) and (1 1 1) Si substrates by the thermal plasma spray CVD method. The intermediate SiO_2 cladding layer thickness was revealed to have no effect on film orientation and crystallinity. It has been demonstrated that substrate temperature is the key factor influencing film orientation and crystallinity; the film direction could be varied from (0 0 6) to (0 1 2) by controlling the deposition temperature. The *c*-axis orientation appears to result from the growth-rate anisotropy effect. Under optimal growth conditions, 97% *c*-textured films could be grown on both thick and very thin intermediate SiO_2 layers. Further experimental studies on nucleation and growth mechanisms are necessary in order to decrease the grain size and improve the surface roughness of the LNT films produced. It is believed that better deposition temperature control and optimal annealing conditions can improve the LNT film crystallinity and optical properties. *c*-Axis oriented LNT films may be very useful in integrated optical devices, pyroelectric devices, and metal-ferroelectric-semiconductor nonvolatile memory applications.

Acknowledgements

We would like to thank Seika Sangyo Ltd., Tokyo, Japan, for their help with the ellipsometric measurements of our samples. We would also like to express our thanks to Mr. H. Nishiyama for his kind assistance in the AFM measurements. S.A.K. is grateful for the support of the Japan Society for the Promotion of Science (JSPS). This work was financially supported by JSPS under the program "Research for the Future" (JSPS-RFTF Grant No. 97R15301).

References

[1] D.K. Fork, F. Armani-Leplingard, J.J. Kingston, MRS Bull. 21 (7) (1996) 53.
[2] X.L. Guo, Z.G. Liu, S.N. Zhu, T. Yu, S.B. Xiong, W.S. Hu, J. Cryst. Growth 165 (1996) 187.
[3] R.S. Weis, T.K. Gaylord, Appl. Phys. A 37 (1985) 191.
[4] A. Räuber, in: E. Kaldis (Ed.), Current Topics in Material Science, Vol. 1, North-Holland, Amsterdam, 1978, p. 481.
[5] M.K. Francombe, S.V. Krishnaswamy, J. Vac. Sci. Technol. A 8 (1990) 1382.
[6] T. Kawaguchi, H. Kitayama, M. Imaeda, S. Ito, K. Kaigawa, T. Taniuchi, T. Fukuda, J. Cryst. Growth 169 (1996) 94.

[7] S.D. Cheng, C.H. Kam, Y. Zhou, X.Q. Han, W.X. Que, Y.L. Lam, Y.C. Chan, J.T. Oh, W.S. Gan, Thin Solid Films 365 (2000) 77.
[8] T. Majima, H. Yamamoto, S.A. Kulinich, K. Terashima, J. Cryst. Growth 220 (2000) 336.
[9] C.H.J. Huang, T.A. Rabson, Opt. Lett. 18 (1993) 811.
[10] D. Ghica, C. Ghica, M. Gartner, V. Nelea, C. Martin, A. Cavaleru, I.N. Mihailescu, Appl. Surf. Sci. 138/139 (1999) 617.
[11] A. Tanaka, K. Miyashita, T. Tashiro, M. Kimura, T. Sukegawa, J. Cryst. Growth 148 (1995) 324.
[12] V.T. Volkov, L.S. Kokhanovchik, V.N. Matveev, S.V. Nosenko, Microelectron. Eng. 29 (1995) 305.
[13] S.D. Cheng, Y. Zhou, C.H. Kam, X.Q. Han, W.X. Que, Y.L. Lam, Y.C. Chan, J.T. Oh, W.S. Gan, Mater. Lett. 44 (2000) 125.
[14] V. Bornand, Ph. Papet, E. Philippot, Thin Solid Films 304 (1997) 239.
[15] X.L. Guo, W.S. Hu, Z.G. Liu, S.N. Zhu, T. Yu, S.B. Xiong, C.Y. Lin, Mater. Sci. Eng. B 53 (1998) 278.
[16] S.Y. Lee, R.S. Feigelson, J. Mater. Res. 14 (1999) 2662.
[17] W.S. Hu, Z.G. Liu, Z.C. Wu, J.M. Liu, X.Y. Chen, D. Feng, Appl. Surf. Sci. 141 (1999) 197.
[18] Z.G. Liu, W.S. Hu, X.L. Guo, J.M. Liu, D. Feng, Appl. Surf. Sci. 109/110 (1997) 520.
[19] N. Yamaguchi, T. Hattori, K. Terashima, T. Yoshida, Thin Solid Films 316 (1998) 185.
[20] H. Yamamoto, S.A. Kulinich, K. Terashima, Thin Solid Films 390 (2001) 1.
[21] D.V. Shtansky, S.A. Kulinich, K. Terashima, T. Yoshida, Y. Ikuhara, J. Mater. Res. 16 (2001) 2271.
[22] Y. Kakehi, A. Okamoto, Y. Sakurai, Y. Nishikawa, T. Yotsuya, S. Ogawa, Appl. Surf. Sci. 169/170 (2001) 560.
[23] S. Tan, T. Gilbert, C.-Y. Hung, T.E. Schlesinger, M. Migliuolo, J. Appl. Phys. 79 (1996) 3548.
[24] Z.C. Wu, W.S. Hu, J.M. Liu, M. Wang, Z.G. Liu, Mater. Lett. 34 (1998) 332.
[25] S.Y. Lee, R.S. Feigelson, J. Cryst. Growth 186 (1998) 594.
[26] D. Xue, K. Betzler, H. Hess, Solid State Commun. 115 (2000) 581.
[27] F. Shimura, J. Cryst. Growth 42 (1977) 579.